Some Mathematical Properties of Morphoelasticity

Egberts, Ginger; Smits, Daan; Vermolen, Fred; van Zuijlen, Paul

DOI
10.1007/978-3-030-55874-1_111

Publication date
2021

Document Version
Final published version

Published in
Numerical Mathematics and Advanced Applications, ENUMATH 2019 - European Conference

Citation (APA)
Egberts, G., Smits, D., Vermolen, F., & van Zuijlen, P. (2021). Some Mathematical Properties of Morphoelasticity. In F. J. Vermolen, & C. Vuik (Eds.), *Numerical Mathematics and Advanced Applications, ENUMATH 2019 - European Conference* (pp. 1119-1127). (Lecture Notes in Computational Science and Engineering; Vol. 139). Springer. https://doi.org/10.1007/978-3-030-55874-1_111

Some Mathematical Properties of Morphoelasticity

Ginger Egberts, Daan Smits, Fred Vermolen, and Paul van Zuijlen

Abstract We consider a morphoelastic framework that models permanent deformations. The text treats a stability assessment in one dimension and a preservation of symmetry in multiple dimensions. Next, we treat the influence of uncertainty in some of the field variables onto the predicted behaviour of tissue.

1 Introduction

Growth phenomena are well-studied topic in (medical) biology. Examples are tumor growth, organ development, embryonic growth or the evolution of skin. Organ development is a very interesting research or futuristic scientific development in which one tries to cultivate human and mammalian organs as an alternative to the need of donors for organ transplantation. In many cases, organs from donors will undergo repellence as a result of the immune system of the host. Therefore development of organs on the basis of the DNA from the host is of scientific interest. Further interest comes from modern meat industry in which meat is to be development outside the animal, such that slaughtering animals is no longer necessary. Of course, these topics are still visionary, however, in the future, these topics are expected to gain further research interest, including breakthroughs, and even will be implemented at a certain stage.

G. Egberts · D. Smits · F. Vermolen (✉)
Delft Institute of Applied Mathematics, Delft University of Technology, Delft, The Netherlands
e-mail: F.J.Vermolen@tudelft.nl

P. van Zuijlen
Department of Plastic, Reconstructive and Hand Surgery, MOVE Research Institute, VU University Medical Centre, Amsterdam, The Netherlands

Burn Centre, Red Cross Hospital, Beverwijk, The Netherlands

Department of Plastic, Reconstructive and Hand Surgery, Red Cross Hospital, Beverwijk, The Netherlands

F. J. Vermolen, C. Vuik (eds.), *Numerical Mathematics and Advanced Applications ENUMATH 2019*, Lecture Notes in Computational Science and Engineering 139, https://doi.org/10.1007/978-3-030-55874-1_111

Mathematical models for growth exist in different levels of complexity, such as growth models that are based on curvature or on surface processes on the boundary of the growing object. Examples are particle growth and phase transitions in grains or the closure of a shallow scrub wound, in which the epidermis (upper skin) grows over the wounded area as a result of localised migration and proliferation of keratinocytes (cells in the epidermis). Other growth processes take place as a result of processes that are happening all over the body of the growing object. In biological applications, one may think of embryonic growth or tumor growth. In all these cases, in-body growth induces mechanical stresses and strains in the body. In large skin wounds, such as serious burn injuries, where skin contraction takes place, the skin may undergo changes such that permanent deformations remain. To deal with these mechanical processes, one composes a balance of momentum and one uses a constitutive law that couples the stresses and strains in the body. If one uses classical elasticity with Hooks's Law, then the deformations will always vanish as the forces are released. Hence growth and/or permanent deformations cannot be predicted with classical mechanical balances only. For this reason, one incorporates growth through morphoelasticity, which was described very clearly by Hall [1] and introduced earlier by Rodriguez et al. [2]. Here, one uses the following principle: the total deformation is decomposed into a deformation as a result of growth and a deformation as a result of mechanical forces. In a mathematical context, one considers the following three coordinate systems: $\mathbf{X}$, $\mathbf{X}_e(t)$, and $\mathbf{x}(t)$, which, respectively, represent the initial coordinate system, the equilibrium at time t that results due to growth or shrinkage, and the current coordinate system that results due to growth or shrinkage and mechanical deformation. The deformation gradient tensor is factorised into $\mathbf{F} = \mathbf{A}\,\mathbf{Z}$: $\mathbf{Z}$ a deformation gradient tensor due to (permanent) growth or shrinkage; and $\mathbf{A}$ a deformation gradient tensor due to (current) mechanical forces.

Another complication that is often encountered in biological systems is the fact that many of the biological variables change from individual to individual. Even changes within the same individual over time and location are not uncommon. These variations, both microscopic (local) and from individual to individual make the biological system suffer from a large degree of uncertainty and therefore many of the biological simulation frameworks should be designed such that they allow the estimation of likelihood that certain scenarios (such as metastasis of tumors or skin contraction after wounding) take place.

As far as we know, the morphoelastic system has not yet been analysed mathematically, and therefore we give some preliminary results for stability and symmetry of the strain tensor. Furthermore, we will show how to quantify the impact of uncertainty in the input parameters on the dynamics of tissue.

2 The Model for Morphoelasticity

Hall [1] derived a set of PDEs that integrate growth/shrinkage with mechanical forces in a two-field formalism for the displacement velocity and the effective Eulerian strain between the current equilibrium configuration and current configuration, based on the deformation gradient tensor $\mathbf{A}$. Let $\frac{D(.)}{Dt}$ denote the material time derivative of a quantify, then we consider the following differential equations for the displacement velocity $\mathbf{v}$ and the effective Eulerian strain $\boldsymbol{\epsilon}$ in an open Lipschitz domain $\Omega(t)$:

$$\begin{aligned} \rho\left(\frac{D\mathbf{v}}{Dt} + \mathbf{v}(\nabla\cdot\mathbf{v})\right) - \nabla\cdot\boldsymbol{\sigma} &= \mathbf{f}, \\ \frac{D\boldsymbol{\epsilon}}{Dt} + \boldsymbol{\epsilon}\,\mathrm{skw}(\mathbf{L}) - \mathrm{skw}(\mathbf{L})\,\boldsymbol{\epsilon} + (\mathrm{tr}(\boldsymbol{\epsilon}) - 1)\mathrm{sym}(\mathbf{L}) &= -\mathbf{G}. \end{aligned} \tag{1}$$

Here $\boldsymbol{\sigma}$, $\mathbf{L}$, $\mathbf{G}$, $\mathbf{f}$, respectively, denote the stress tensor, deformation gradient velocity tensor, growth tensor and body force that are given by

$$\begin{aligned} \mathbf{L} = \nabla\mathbf{v}, \quad \mathbf{G} = \alpha\boldsymbol{\epsilon}, \qquad \alpha \in \mathbb{R}, \\ \boldsymbol{\sigma} = \mu_1\mathrm{sym}(\mathbf{L}) + \mu_2\mathrm{tr}(\mathrm{sym}(\mathbf{L}))\mathbf{I} + \frac{E}{1+\nu}\left(\boldsymbol{\epsilon} + \frac{\nu}{1-2\nu}\mathrm{tr}(\boldsymbol{\epsilon})\mathbf{I}\right). \end{aligned} \tag{2}$$

Here E, μ_1, μ_2, ν, respectively, represent the Youngs modulus (stiffness), kinematic and dynamic viscosity and Poisson ratio. Further, sym($\mathbf{L}$) and skw($\mathbf{L}$), respectively, denote the symmetric and skew-symmetric part of the tensor L. Equations (1) are solved for $\mathbf{v}$ and $\boldsymbol{\epsilon}$, and need boundary conditions for $\mathbf{v}$ and initial conditions for both $\mathbf{v}$ and $\boldsymbol{\epsilon}$. The displacement is postprocessed by integration of $\mathbf{v}$ over t.

3 Symmetry and Stability

3.1 Symmetry of the Strain Tensor

First, we demonstrate that if the strain tensor $\boldsymbol{\epsilon}$ is initially symmetric then it remains symmetric at all later times.

Theorem 1 *Let the second equation in Eq. (1) hold on open Lipschitz domain* Ω *for* $t > 0$*, suppose that* $\boldsymbol{\epsilon}$ *is symmetric on* $t = 0$*, then* $\boldsymbol{\epsilon}$ *remains symmetric for* $t > 0$*.*

Proof Taking the transpose of the second equation in Eq. (1), gives

$$\begin{aligned} \frac{D\boldsymbol{\epsilon}}{Dt} + \boldsymbol{\epsilon}\,\mathrm{skw}(\mathbf{L}) - \mathrm{skw}(\mathbf{L})\,\boldsymbol{\epsilon} + (\mathrm{tr}(\boldsymbol{\epsilon}) - 1)\mathrm{sym}(\mathbf{L}) &= -\alpha\boldsymbol{\epsilon}, \\ \frac{D\boldsymbol{\epsilon}^T}{Dt} + \boldsymbol{\epsilon}^T\,\mathrm{skw}(\mathbf{L}) - \mathrm{skw}(\mathbf{L})\,\boldsymbol{\epsilon}^T + (\mathrm{tr}(\boldsymbol{\epsilon}) - 1)\mathrm{sym}(\mathbf{L}) &= -\alpha\boldsymbol{\epsilon}^T. \end{aligned} \tag{3}$$

Note that we used $\mathrm{sym}(\mathbf{L})^T = \mathrm{sym}(\mathbf{L})$ and $\mathrm{skw}(\mathbf{L})^T = -\mathrm{skw}(\mathbf{L})$, subtraction gives

$$\frac{D}{Dt}(\boldsymbol{\epsilon} - \boldsymbol{\epsilon}^T) + (\boldsymbol{\epsilon} - \boldsymbol{\epsilon}^T)\,\mathrm{skw}(\mathbf{L}) - \mathrm{skw}(\mathbf{L})\,(\boldsymbol{\epsilon} - \boldsymbol{\epsilon}^T) = -\alpha(\boldsymbol{\epsilon} - \boldsymbol{\epsilon}^T). \tag{4}$$

From the above equation, it is clear that $(\boldsymbol{\epsilon} - \boldsymbol{\epsilon}^T) = \mathbf{0}$ represents an equilibrium, and hence symmetry of $\boldsymbol{\epsilon}$ represents an equilibrium, by which we conclude that initial symmetry implies no changes of symmetry for later times. □

The actual stability of this symmetry is another question worth investigating. We postpone this matter to future studies. Symmetry of the strain tensor warrants symmetry of the stress tensor, see Eq. (2), which implies zero torque and hence there is no spin.

3.2 Linear Stability of 1D Morphoelasticity

Next we consider the one-dimensional counterpart of Eqs. (1), which after processing the material time derivative, is given by

$$\begin{aligned} \rho\left(\frac{\partial v}{\partial t} + 2v\frac{\partial v}{\partial x}\right) - \mu\frac{\partial^2 v}{\partial x^2} - E\frac{\partial \epsilon}{\partial x} &= f, \\ \frac{\partial \epsilon}{\partial t} + v\frac{\partial \epsilon}{\partial x} + (\epsilon - 1)\frac{\partial v}{\partial x} &= -G. \end{aligned} \tag{5}$$

The domain is given by $\Omega(t) = (0, 1)$ where we use $v(t, 0) = v(t, 1) = 0$ as boundary conditions, which implies that the domain is fixed and that deformations can only form locally. We analyse stability of constant states in the above one-dimensional problem. To this extent, we analyse perturbations around the equilibria $v = 0$ and $\epsilon = \epsilon_0 \in \mathbb{R}$ for the case that $f = 0$ and $G = 0$. Linearisation of the above equations around these equilibria, gives

$$\rho\frac{\partial \tilde{v}}{\partial t} - \mu\frac{\partial^2 \tilde{v}}{\partial x^2} - E\frac{\partial \tilde{\epsilon}}{\partial x} = 0, \qquad \frac{\partial \tilde{\epsilon}}{\partial t} + (\epsilon_0 - 1)\frac{\partial \tilde{v}}{\partial x} = 0, \tag{6}$$

where $\tilde{v}$ and $\tilde{\epsilon}$ are perturbations around $v = 0$ and $\epsilon = \epsilon_0$. We write the perturbations in terms of a complex Fourier series, that is, we set

$$\tilde{v}(t,x) = \sum_{j=-\infty}^{\infty} c_j^v(t) e^{2i\pi jx}, \qquad \tilde{\epsilon}(t,x) = \epsilon_0 + \sum_{j=-\infty}^{\infty} c_j^\epsilon(t) e^{2i\pi jx}, \tag{7}$$

where we are to find coefficients c_j^v and c_j^ϵ, and where i represents the imaginary unit number. The use of Fourier Series for stability assessment was also described in, among others, [3]. Substitution into Eqs. (6), gives

$$\begin{aligned} \rho \sum_{j=-\infty}^{\infty} \dot{c}_j^v(t) e^{2i\pi jx} + \mu \sum_{j=\infty}^{\infty} (2\pi j)^2 c_j^v(t) e^{2i\pi jx} - iE \sum_{j=-\infty}^{\infty} (2\pi j) c_j^\epsilon(t) e^{2i\pi jx} = 0, \\ \sum_{j=-\infty}^{\infty} \dot{c}_j^\epsilon(t) e^{2i\pi jx} + i(\epsilon_0 - 1) \sum_{j=\infty}^{\infty} (2\pi j) c_j^v(t) e^{2i\pi jx} = 0. \end{aligned} \tag{8}$$

Orthonormality over $\Omega = (0,1)$, implies after multiplication by $e^{-2i\pi kx}$ and integration over Ω that

$$\begin{aligned} \dot{c}_k^v(t) + \frac{(2\pi k)^2 \mu}{\rho} c_k^v(t) - i\, \frac{2\pi k E}{\rho} c_k^\epsilon(t) = 0, \\ \dot{c}_k^\epsilon(t) + i\, 2\pi k(\epsilon_0 - 1) c_k^v(t) = 0. \end{aligned} \tag{9}$$

The above equations are in the form $y' + Ay = 0$, then $A = \begin{pmatrix} \frac{(2\pi k)^2 \mu}{\rho} & -i\frac{2\pi kE}{\rho} \\ i(\epsilon_0 - 1)2\pi k & 0 \end{pmatrix}$. This matrix has the following eigenvalues

$$\lambda_\pm = \frac{(2\pi k)^2 \mu}{2\rho} \pm \frac{1}{2} \sqrt{(\frac{(2\pi k)^2 \mu}{\rho})^2 + 4 \frac{(2\pi k)^2 E}{\rho} (\epsilon_0 - 1)}.$$

This implies that linear stability is obtained for $\epsilon_0 \leq 1$, else a saddle point problem is obtained if $\lambda_\pm \in \mathbb{R}$. The eigenvalues are real-valued as long as $\mu \geq \frac{\sqrt{\rho E(1-\epsilon_0)}}{\pi}$ $(k = 1)$. The constant case $k = 0$ implies $\lambda_\pm = 0$, which reflects the trivial case in which there is no dynamics. This also implies that $\epsilon_0 = 0$ is a stable equilibrium state. Next to this, integration of Eqs. (6) over Ω, gives

$$\begin{aligned} \rho \frac{d}{dt} \int_0^1 \tilde{v} dx = \left[\mu \frac{\partial \tilde{v}}{\partial x} + E\tilde{\epsilon} \right]_0^1, \\ \frac{d}{dt} \int_0^1 \tilde{\epsilon} dx + (\epsilon_0 - 1) \left[\tilde{v} \right]_0^1 = 0 \Longrightarrow \frac{d}{dt} \int_0^1 \tilde{\epsilon} dx = 0 \Longrightarrow \int_0^1 \tilde{\epsilon} dx = \epsilon_0. \end{aligned} \tag{10}$$

Note that the boundary conditions $v(0,t) = v(1,t) = 0$ have been used in the second relation of the above equations. The solution $\tilde{\epsilon}$ to Eq. (6) converges towards ϵ_0 under conservation of $\tilde{\epsilon}$ such that $\epsilon_0 = \int_0^1 \tilde{\epsilon}(0,x)dx$. We summarise these results in Theorem 2, where we remark that one easily generalises the observations to a generic fixed domain $\Omega \subset \mathbb{R}$:

Theorem 2 *Let (v,ϵ) satisfy Eqs. (5), under the boundary conditions that $v = 0$ on the boundaries of open, connected domain $\Omega \subset \mathbb{R}$, then*

1. *The equilibria $(v,\epsilon) = (0,\epsilon_0)$, $\epsilon_0 \in \mathbb{R}$, are linearly stable if and only if $\epsilon_0 < 1$;*
2. *Given $\epsilon_0 < 1$, then the eigenvalues are real-valued if and only if $\mu \geq \frac{\sqrt{\rho E(1-\epsilon_0)}}{\pi}|\Omega|$ $(k = 1)$, where $|\Omega|$ denotes the size (measure) of Ω;*
3. *Convergence takes place through $\epsilon_0|\Omega| = \int_\Omega \tilde{\epsilon}(0,x)dx$;*

If $\epsilon_0 < 1$ and if $\mu < \frac{\sqrt{\rho E(1-\epsilon_0)}}{\pi}|\Omega|$ then convergence from perturbations around ϵ_0 will occur in a nonmonotonic way over time due to the fact that the eigenvalues of the linearised dynamical system are not real-valued. Furthermore, if $G = \alpha\epsilon$ for $\alpha > 0$, then the only stable equilibrium is $(v,\epsilon) = (0,0)$.

4 Computer Simulations

First the numerical method and typical results are briefly explained. This is followed by results from a stochastic stiffness.

4.1 The Numerical Method and Typical Results

The solution to the model equations (1) and (2) is approximated by the finite-element method using linear triangles. Time integration is done by backward Euler in which a monolithic approach is used with Picard inner iterations. In cases that the triangles become ill-shaped, remeshing is applied. In three dimensions, the same is done for linear tetrahedra and bricks. A more detailed treatment is beyond the scope of the current paper, and can be found in [4]. We consider the example of a contracting wound. The results have been shown in Fig. 1, in which the left plot displays the area of a wound that first contracts due to cellular (fibroblast) forces, and subsequently retracts due to the release of cellular forces. In the case of viscoelasticity, it can be seen that the retraction proceeds until the boundaries coincide with the initial boundaries. It can also be seen that morphoelasticity predicts a permanent deformation in the sense that the area of the inflicted region does not converge to the initial configuration. The plot on the right shows how the maximum displacement and the dynamic equilibrium (due to deformation gradient tensor Z) evolves.

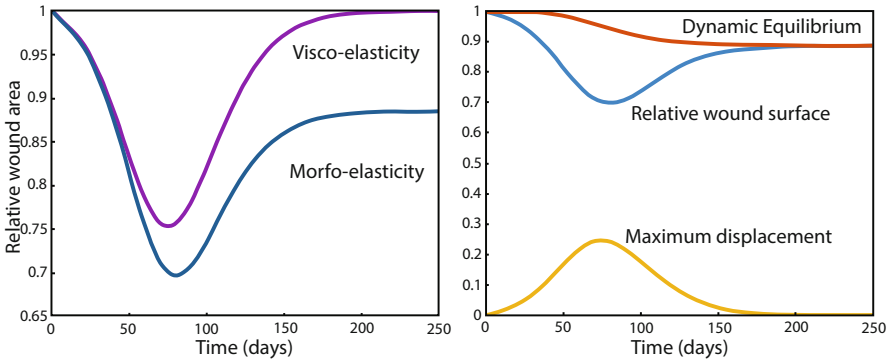

Fig. 1 Left: the relative wound area over time using the viscoelastic approach and morphoelastic approach; Right: the morphoelastic approach with the wound area, equilibrium and maximum displacement as a function of time

4.2 Quantification of Uncertainty

Since tissues contain unpredictable spatial microscopic variations, we assume that E, ρ, forcing f and α are random field variables over X consisting of lognormally distributed perturbations around their means. The fields of the aforementioned parameters are obtained through the following truncated Karhunen-Loève expansion over the spatial variable X

$$\hat{u}(X) = \sum_{j=1}^{n} \hat{Z}_j \sqrt{\frac{2}{n}} \sin((2j-1)\frac{\pi}{2L}X), \text{ where } \hat{Z}_j \sim \mathcal{N}(0,1).$$

Here $\hat{Z}_j$ defines a set of *iid* stochastic variables that follow the standard normal distribution. The stochastic field variable $\hat{u}(X)$ is used to evaluate the field variables E, ρ, f and α. We explain the regeneration procedure for $\hat{E}(X)$:

$$\log(\hat{E}(X)) = \mu_E + \sigma_E \hat{u}(X) \Longrightarrow \hat{E}(X) = \exp(\mu + \sigma \hat{u}(X)),$$

where μ_E and σ_E^2 are the mean (expected value) and variance of $\hat{E}$. The mean and variance are related to the *arithmetic* sample mean $\mathcal{M}$ and *arithmetic* sample standard deviation $\mathcal{S}$ by

$$\mu_E = \ln(\frac{\mathcal{M}^2}{\sqrt{1+\frac{\mathcal{S}^2}{\mathcal{M}^2}}}), \text{ and } \sigma_E = \sqrt{\ln(1+\frac{\mathcal{S}^2}{\mathcal{M}^2})}. \tag{11}$$

Figure 2 shows histograms and an estimated cumulative probability distribution for the minimal reduction of area and the final reduction of area after having computed

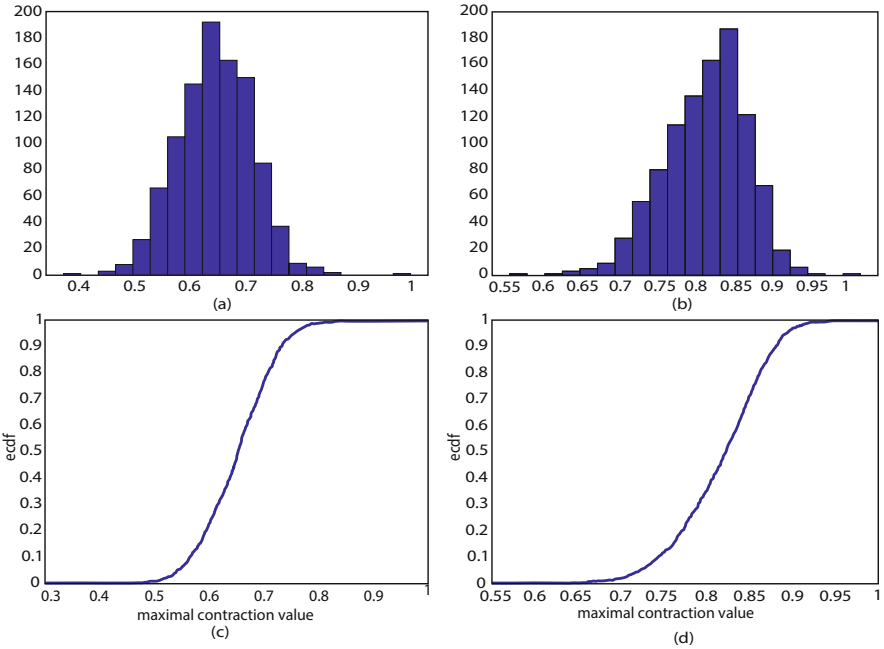

Fig. 2 Results from 1000 samples with $\mathcal{M}_E = 31$ N/(g cm)$^{1/2}$, $\mathcal{S}_E = 11$, $\mathcal{M}_\mu = 10^2$ (N day)/cm, $\mathcal{S}_\mu = 1$, $\mathcal{M}_\rho = 1.02$ g/cm, $\mathcal{S}_\rho = 0.2$, $\mathcal{M}_f = 4$ N/cm, $\mathcal{S}_f = 2$, $\mathcal{M}_\alpha = 0.05$ $(-)$, $\mathcal{S}_\alpha = 0.02$, (**a**) histogram of the maximum wound contraction, that is the minimal wound area; (**b**) histogram of the final contraction, that is the final wound area; (**c**) cumulated probability density for the minimal wound area; (**d**) cumulated probability density for the final wound area

1000 samples. From Fig. 2 the likelihood that the contraction is worse than a certain threshold can be estimated. For instance, from Fig. 2d, the likelihood that the final wound area is smaller than 80% of its original value is about 0.28 (28%).

5 Conclusions

We have shown that morphoelasticity in combination with linear Hooke's Law implies that if the Eulerian effective strain tensor is initially symmetric, then it remains symmetric at all later times. Further, a stability analysis for the one-dimensional case revealed that all Eulerian effective strains smaller than one in combination with zero displacement velocity, represent linearly stable states. Further a condition for monotonicity of convergence over time has been derived. Next to these issues, a Karhunen-Loève expansion has been used for several variables involved to estimate the likelihood that contraction exceed a certain threshold. The model is subject to further uncertainty quantification.

Acknowledgments The authors are grateful for the financial support by the Dutch Burns Foundation under Project 17.105. Furthermore, the suggestions from the referee to improve the presentation of the manuscript are also warmly acknowledged.

References

1. Hall, C.L.: Modelling of some biological materials using continuum mechanics. PhD-thesis at the Queensland University of Technology (2008)
2. Rodriguez E., Hoger A., McCulloch A.: Stress-dependent finite growth in soft elastic tissues. J Biomech 27, 455–467 (1994)
3. Prokharau, P., Vermolen, F.J.: Stability analysis for a peri-implant osseointegration model. J. Math. Biol, 66, 351–382 (2013)
4. Koppenol, D.C., Vermolen, F.J.: Biomedical implications from a morphoelastic continuum model for the simulation of contracture formation in skin-grafts that cover excised burns. Biomech Model Mechanobiol, 16 (4), 1187–1206 (2017)